

# A cold neutron star in the transient low-mass X-ray binary HETE J1900.1–2455 after 10 years of active accretion

N. Degenaar<sup>1,2\*</sup>, L.S. Ootes<sup>2</sup>, M.T. Reynolds<sup>3</sup>, R. Wijnands<sup>2</sup>, and D. Page<sup>4</sup>

<sup>1</sup>*Institute of Astronomy, University of Cambridge, Madingley Road, Cambridge CB3 0HA, UK*

<sup>2</sup>*Anton Pannekoek Institute for Astronomy, University of Amsterdam, Science Park 904, 1098 XH, Amsterdam, the Netherlands*

<sup>3</sup>*Department of Astronomy, University of Michigan, 1085 South University Avenue, Ann Arbor, MI 48109, USA*

<sup>4</sup>*Instituto de Astronomía, Universidad Nacional Autónoma de México, Mexico D.F. 04510, Mexico*

Accepted 2016 September 23. Received 2016 September 23; in original form 2016 July 12

## ABSTRACT

The neutron star low-mass X-ray binary and intermittent millisecond X-ray pulsar HETE J1900.1–2455 returned to quiescence in late 2015, after a prolonged accretion outburst of  $\simeq 10$  yr. Using a *Chandra* observation taken  $\simeq 180$  d into quiescence we detect the source at a luminosity of  $\simeq 4.5 \times 10^{31} (D/4.7 \text{ kpc})^2 \text{ erg s}^{-1}$  (0.5–10 keV). The X-ray spectrum can be described by a neutron star atmosphere model with a temperature of  $\simeq 54$  eV for an observer at infinity. We perform thermal evolution calculations based on the 2016 quiescent data and a  $\lesssim 98$  eV temperature upper limit inferred from a *Swift* observation taken during an unusually brief ( $\lesssim 2$  weeks) quiescent episode in 2007. We find no evidence in the present data that the thermal properties of the crust, such as the heating rate and thermal conductivity, are different than those of non-pulsating neutron stars. Finding this neutron star so cold after its long outburst imposes interesting constraints on the heat capacity of the stellar core; these become even stronger if further cooling were to occur.

**Key words:** stars: neutron - X-rays: binaries - pulsars: individual (HETE J1900.1–2455)

## 1 INTRODUCTION

Neutron stars are one of the possible remnants of once massive stars that ended their life in a supernova explosion. A defining property of neutron stars is that they are very compact; despite having a mass of  $\simeq 1.4 M_{\odot}$ , their radius is only  $\simeq 10$  km. As a result, their interior density rises beyond the density of atomic nuclei. Neutron stars are therefore of prime interest to understand the properties of ultra-dense matter (e.g. Lattimer 2011, for a review).

Our Galaxy harbors  $>100$  neutron stars that are part of low-mass X-ray binaries (LMXBs) and accrete gas from a  $\lesssim 1 M_{\odot}$  companion star via an accretion disk. Many of these systems are transient; during X-ray luminous phases matter is rapidly falling toward the neutron star, but during intervening quiescent phases the accretion rate, and hence the X-ray luminosity, is strongly reduced. Two sub-classes of neutron star LMXBs are the quasi-persistent sources and the accreting millisecond X-ray pulsars (AMXPs). Each make up  $\simeq 10$  per cent of the current population of neutron star LMXBs, and each have distinct outburst and quiescent properties.

Quasi-persistent LMXBs stand out by showing prolonged accretion outbursts of years to decades rather than weeks to months. Moreover, several of these sources show strong thermal emission in quiescence that gradually decreases on a timescale of years (e.g. Cackett et al. 2013; Fridriksson et al. 2011; Degenaar et al. 2014;

Homan et al. 2014; Merritt et al. 2016). The crust of a neutron star is heated during accretion outbursts via pycnonuclear fusion reactions that take place at  $\simeq 1$  km depth, and electron captures occurring at shallower depth. Together, these processes deposit an energy  $\simeq 1 - 2$  MeV per accreted nucleon, heating the crust (e.g. Haensel & Zdunik 1990, 2008; Brown et al. 1998). The temperature evolution in quiescence of five quasi-persistent sources can be successfully explained as cooling of the strongly-heated neutron star crust and offers valuable insight into the structure and composition of these neutron stars (e.g. Rutledge et al. 2002; Wijnands et al. 2002, 2004; Shternin et al. 2007; Brown & Cumming 2009; Page & Reddy 2013; Medin & Cumming 2014; Deibel et al. 2015; Horowitz et al. 2015; Turlione et al. 2015; Cumming et al. 2016).<sup>1</sup>

AMXPs distinguish themselves by displaying coherent X-ray pulsations when accreting (e.g. Wijnands & van der Klis 1998). It is believed that in these objects the stellar magnetic field is strong enough to disrupt the accretion flow and channel plasma to the magnetic poles of the rapidly rotating neutron star. In quiescence, the persistently-pulsating AMXPs show weak or no thermal X-rays but strong power-law emission (e.g. Campana et al. 2005, 2008; Jonker et al. 2005; Wijnands et al. 2005b; Heinke et al. 2009; Degenaar et al. 2012). Such a hard emission component is also seen in the quiescent spectra of some non-pulsating neutron

<sup>1</sup> Recent studies have also revealed crust cooling in three neutron stars with short outbursts (e.g. Degenaar et al. 2011a, 2015; Waterhouse et al. 2016).

\* e-mail: degenaar@ast.cam.ac.uk

star LMXBs, though it is typically much less prominent. The hard quiescent X-rays are often ascribed to residual accretion or non-thermal emission processes related to the neutron star magnetic field (e.g. Campana et al. 1998; Rutledge et al. 2001; Degenaar et al. 2012; Chakrabarty et al. 2014; Wijnands et al. 2015).

HETE J1900.1–2455 shares properties of both the aforementioned sub-classes of neutron star LMXBs; it is the only known AMXP that accreted for a full decade, and the only quasi-persistent source that acted as an AMXP. The source was first seen in outburst in 2005 June when it exhibited a thermonuclear X-ray burst (Vanderspek et al. 2005). X-ray pulsations at a frequency of 377.3 Hz were soon found, but were detected only sporadically after  $\simeq 2$  months (Galloway et al. 2008b; Patruno 2012). The source is therefore referred to as an “intermittent AMXP”. X-ray burst analysis suggests a source distance of  $D = 4.7$  kpc (Galloway et al. 2008a).

The  $\simeq 10$ -year long outburst of HETE J1900.1–2455 ended in late 2015. We report on a *Chandra* ToO observation obtained  $\simeq 180$  d after it went quiescent. We combine the obtained temperature measurement with an upper limit from *Swift* in 2007 when the source disappeared for  $\lesssim 2$  weeks, to perform thermal evolution simulations and to probe the thermal properties of this neutron star.

## 2 OBSERVATIONS AND DATA ANALYSIS

We performed spectral fits in XSPEC (v. 12.9). Interstellar absorption was included by using TBABS with VERN cross-sections (Verner et al. 1996) and WILM abundances (Wilms et al. 2000). Fluxes were calculated using CFLUX. Quoted errors reflect  $1\sigma$  confidence intervals and upper limits are given at 95% confidence level.

### 2.1 *Chandra* quiescence observation in 2016

We observed HETE J1900.1–2455 with *Chandra* for  $\simeq 29.7$  ks from 2016 April 18 at 21:50 UT till April 19 at 06:48 UT. The source was placed on the ACIS S-3 chip, which was operated in very faint, timed mode. We reduced and analyzed the data using CIAO v. 4.8. Source events were extracted from a circular region with a radius of  $2''$  and a surrounding source-free annulus with an inner–outer radius of  $5''$ – $25''$  was used for the background. The source was detected at a net count rate of  $(2.36 \pm 0.03) \times 10^{-3}$  c s $^{-1}$ , yielding a total of 70 source photons. Spectra and response files were extracted using SPECEXTRACT. We grouped the spectral data to  $>1$  counts bin $^{-1}$  using GRPPHA and then fitted the data in the 0.3–7 keV range applying W-statistics (i.e. Cash-statistics with background subtraction; Wachter et al. 1979).

### 2.2 *Swift*/XRT non-detections in 2007 and 2016

Between 2016 March 7 and April 9, *Swift* observed HETE J1900.1–2455 several times with the XRT in photon counting mode (ObsID 00030946021–27). We use these observations, with exposure times of  $\simeq 0.9$ – $1.1$  ks, to obtain constraints on the neutron star temperature prior to our *Chandra* observation. We also re-analyze a single 0.8 ks exposure obtained on 2007 June 5 (obsID 00030946002; Degenaar et al. 2007b). None of these *Swift* observations detected the source. The XRT data were analyzed using standard tools incorporated in HEASOFT (v. 6.18). The data were first reduced using the reprocessing pipeline and then examined using XSELECT. Ancillary response files were created using XRTMKARF, and the response matrix file (v. 15) was obtained from the calibration data base.

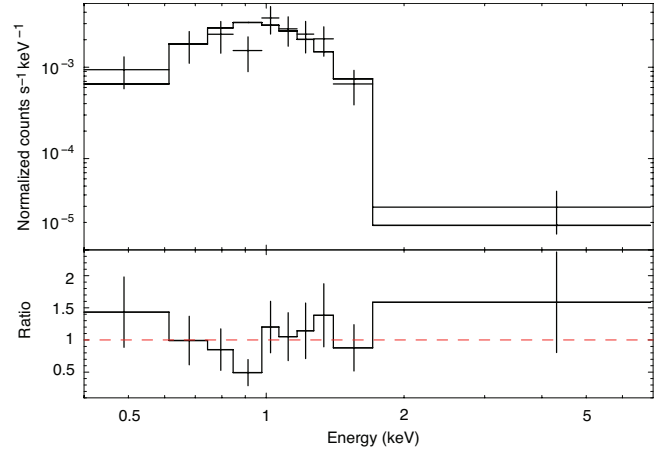


**Figure 1.** *Chandra* spectral data and fit to TBABS\*NSATMOS (rebinned for visual clarity). The lower panel shows the data to model ratio.

## 3 OBSERVATIONAL RESULTS

### 3.1 *Chandra*: A thermal spectrum and a cold neutron star

When fitting the *Chandra* spectral data with a simple power-law model (PEGPWRLW), we obtain an extremely steep index of  $\Gamma = 5.2 \pm 0.9$ . This suggests that the spectrum has a soft, thermal shape. We therefore modeled the spectral data with a physically-motivated neutron star atmosphere model, for which we chose NSATMOS (Heinke et al. 2006). In this model we fixed  $M = 1.4 M_{\odot}$ ,  $R = 10$  km,  $D = 4.7$  kpc and assumed that the entire surface was emitting (i.e. the normalization was set to 1). We note that due to the low flux, we cannot determine the presence of hotspots, which would result in an overestimate of the neutron star surface temperature (e.g. Elshamouty et al. 2016).

The NSATMOS model can adequately describe the spectral data, as is shown in Figure 1. We find  $N_{\text{H}} = (2.2 \pm 0.7) \times 10^{21}$  cm $^{-2}$  and measure a neutron star temperature, as seen by an observer at infinity, of  $kT_{\text{eff}}^{\infty} = 54.4 \pm 1.7$  eV. The inferred 0.5–10 keV flux of  $F_{\text{X}} = (1.7 \pm 0.8) \times 10^{-14}$  erg cm $^{-2}$  s $^{-1}$  translates into a luminosity of  $L_{\text{X}} = (4.5 \pm 2.1) \times 10^{31}$  erg s $^{-1}$  at 4.7 kpc. We estimate a thermal bolometric flux of  $F_{\text{bol}}^{\text{q}} = (2.3 \pm 1.4) \times 10^{-14}$  erg cm $^{-2}$  s $^{-1}$  by extrapolating the fit to the 0.01–100 keV range, which yields  $L_{\text{bol}}^{\text{q}} = (6.1 \pm 3.7) \times 10^{31}$  erg s $^{-1}$ .

To set an upper limit on the contribution from a hard emission tail, we added a power-law component (PEGPWRLW) to our spectral model. Given the few counts, we fixed the power-law index to  $\Gamma = 1$  and 2. This suggests that any hard spectral component contributes  $\lesssim 9$  per cent to the total unabsorbed 0.5–10 keV flux. For these fits the neutron star temperature decreases by  $\simeq 1$  eV.

### 3.2 *Swift*: Temperature upper limits in quiescence

For each *Swift*/XRT non-detection we counted the number of photons in a circular  $10''$  region centered on the source position and calculated a 95% confidence upper limit by using the tables of Gehrels (1986). For each data set we simulated NSATMOS spectra with  $D = 4.7$  kpc,  $M = 1.4 M_{\odot}$ ,  $R = 10$  km,  $N_{\text{H}} = 2 \times 10^{21}$  cm $^{-2}$ , and different temperatures, using the observation-specific response files. A temperature upper limit was then estimated by matching the determined XRT count rate upper limit with that predicted by the simulated spectra.

We obtain  $kT_{\text{eff}}^{\infty} \lesssim 72 - 93$  eV for the different *Swift*

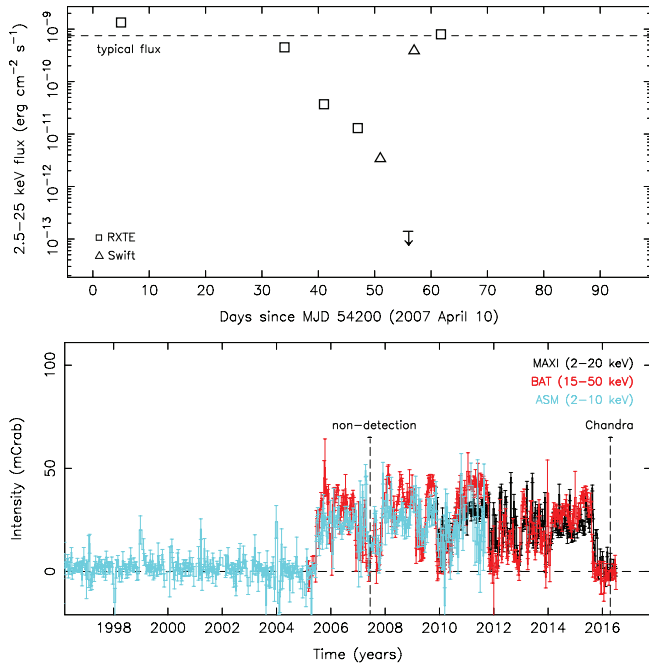


**Figure 2.** Light curves of HETE J1900.1–2455. Top: Combined *RXTE*/PCA and *Swift*/XRT light curve in 2007 April–June (fluxes from Galloway et al. 2007; Degenaar et al. 2007a,c,b). Bottom: *RXTE*/ASM, *Swift*/BAT, and *MAXI* monitoring data binned per 10 days.

observations of 2016. The corresponding upper limits on the 0.5–10 keV unabsorbed fluxes and luminosities are  $F_X \lesssim (1 - 4) \times 10^{-13} \text{ erg cm}^{-2} \text{ s}^{-1}$  and  $L_X \lesssim (2.6 - 10.6) \times 10^{32} (D/4.7 \text{ kpc})^2 \text{ erg s}^{-1}$ , respectively. Summing all XRT data (6.5 ks) results in a non-detection that suggests  $kT_{\text{eff}}^{\infty} \lesssim 63 \text{ eV}$  and  $F_X \lesssim 6 \times 10^{-14} \text{ erg cm}^{-2} \text{ s}^{-1}$ .

In 2007 May, the flux of HETE J1900.1–2455 decayed from its regular outburst level by  $>2$  orders of magnitudes in  $\simeq 22 \text{ d}$  (Galloway et al. 2007; Degenaar et al. 2007a), leading to a non-detection with *Swift*/XRT on June 5 (Degenaar et al. 2007b). Only  $\simeq 5 \text{ d}$  later, however, the source was found back at its outburst level (Degenaar et al. 2007c). The light curve constructed from reported *RXTE*/PCA and *Swift*/XRT observations is shown in Figure 2 (top).

From the 2007 *Swift*/XRT non-detection we infer  $kT_{\text{eff}}^{\infty} \lesssim 98 \text{ eV}$ ,  $F_X \lesssim 5.2 \times 10^{-13} \text{ erg cm}^{-2} \text{ s}^{-1}$  and  $L_X \lesssim 1.4 \times 10^{33} (D/4.7 \text{ kpc})^2 \text{ erg s}^{-1}$  (0.5–10 keV). On May 31, the X-ray spectrum could be fitted by a power-law model with  $\Gamma \simeq 2.5$ , suggesting that the source was still accreting at that time (Degenaar et al. 2007a). The non-detection could thus not have been more than 7 d into quiescence, and the total off-time no longer than  $\simeq 11 \text{ d}$ .

#### 4 THERMAL EVOLUTION SIMULATIONS

Thermal evolution models can be employed to study how the crust of neutron stars is heated during accretion outbursts and subsequently cools in quiescence. We use the code NSCOOL (Page & Reddy 2013), expanded with a new module to incorporate outburst flux variations (Ootes et al. 2016). For details we refer to Page & Reddy (2013) and Ootes et al. (2016); here we only discuss the source-specific input. In all our simulations, we require the crust temperature to be consistent with both the 2016 *Chandra* and *Swift* data, as well as the 2007 *Swift* upper limit. For consistency with our spectral analysis, we assumed  $M = 1.4 M_{\odot}$  and  $R = 10 \text{ km}$ .

For the outburst properties, we used the publicly available light curves from the *RXTE*/ASM (2–10 keV), *MAXI* (2–20 keV; Matsuoka et al. 2009), and *Swift*/BAT (15–50 keV; Krimm et al. 2013), which are shown in Figure 2 (bottom). The instrument count rates were first converted to Crab units and then to bolometric fluxes ( $F_{\text{bol}}^{\text{ob}}$ ) assuming a correction factor of  $c_{\text{bol}} = 2$  (Galloway et al. 2008a). The mass-accretion rate was then calculated as  $\dot{M} = 4\pi D^2 F_{\text{bol}}^{\text{ob}} / \eta c^2$ , where we assumed an accretion efficiency of  $\eta = 0.2$ . This way we estimate an outburst-averaged value of  $\langle \dot{M} \rangle \simeq 3.7 \times 10^{-10} M_{\odot} \text{ yr}^{-1} (\simeq 2.3 \times 10^{16} \text{ g s}^{-1})$ . The source was not detected in daily *MAXI* scans after 2015 October 20, implying  $L_X \lesssim 5 \times 10^{35} (D/4.7 \text{ kpc})^2 \text{ erg s}^{-1}$  (2–20 keV). Based on the rapid flux decay observed in 2007 (Figure 2 top), it is plausible that the source entered quiescence quickly after this. We therefore tentatively set the onset of quiescence,  $t_0$ , to MJD 57321.

The free parameters in our simulations are the temperature of the neutron star core, which red-shifted value (i.e. in the observer frame) we denote as  $\tilde{T}_0$ , and the thermal conductivity of the crust. The latter is parametrized by the level of impurities  $Q_{\text{imp}}$ , where a higher  $Q_{\text{imp}}$  implies a lower conductivity. Furthermore, we allow for the presence of a source of shallow heat, characterized by a depth  $\rho_{\text{sh}}$  and a strength of  $Q_{\text{sh}}$ , in addition to the energy released in standard nuclear heating reactions. A shallow heat source, with a typical magnitude of  $Q_{\text{sh}} \simeq 1 - 2 \text{ MeV}$  and one extreme case of  $Q_{\text{sh}} \simeq 6 - 16 \text{ MeV}$  per accreted nucleon, has been inferred for several neutron stars although its origin remains unknown (e.g. Brown & Cumming 2009; Degenaar et al. 2011a; Deibel et al. 2015; Ootes et al. 2016; Waterhouse et al. 2016). We set  $\rho_{\text{sh}} = 4 \times 10^8 \text{ g cm}^{-3}$  as determined from modeling the crust cooling curve of KS 1731–260 (Ootes et al. 2016), but allowed for different values of  $Q_{\text{sh}}$ .

We assumed the presence of a thick layer of light elements in the neutron star envelope at a column depth of  $y_L \sim 10^9 \text{ g cm}^{-2}$ , following the models of Potekhin et al. (1997). For a hot star the value of  $y_L$  can have a significant effect on the inferred temperature  $\tilde{T}_0$ , up to a factor four, and a series of possible set-ups are shown in Figure 3 (right). For our low temperature of  $kT_{\text{eff}}^{\infty} \simeq 54 \text{ eV}$  (dotted line), any  $y_L > 10^9 \text{ g cm}^{-2}$  gives  $\tilde{T}_0 \simeq 2 \times 10^7 \text{ K}$ . If  $y_L$  is much smaller than we assume here,  $\tilde{T}_0$  could be higher by up to a factor 2. However, if further cooling occurs, the assumed value of  $y_L$  becomes less important; for  $kT_{\text{eff}}^{\infty} \lesssim 30 \text{ eV}$  the inferred  $\tilde{T}_0$  is practically independent of  $y_L$  (see Figure 3 right).

Motivated by crust cooling modeling of other neutron stars (e.g. Brown & Cumming 2009; Page & Reddy 2013; Ootes et al. 2016), we started our simulations with  $Q_{\text{imp}} = 1$  both with and without shallow heating (solid and dashed-dotted curves in Figure 3 left and middle). We find that the crust of the neutron star then cools rapidly, within  $\simeq 200 \text{ days}$ . Without a shallow heat source (dashed-dotted curve) the crust is hardly heated due to the low outburst accretion rate. The current data allow for the presence of a shallow heat source up to  $Q_{\text{sh}} \simeq 3 \text{ MeV}$  (solid curve). We note, however, that for this amount of shallow heating the temperature in 2007 is only just consistent with the *Swift* upper limit (Figure 3 left). For these two models the red-shifted core temperature is  $\tilde{T}_0 = (1.8 - 2.4) \times 10^7 \text{ K}$ , corresponding to a final temperature of  $kT_{\text{eff}}^{\infty} \simeq 46 - 53 \text{ eV}$ , i.e. close to our *Chandra* measurement. With  $Q_{\text{imp}} = 1$ , the *Chandra* point cannot be fitted with a much lower core temperature, hence hardly any further cooling is expected.

A higher crust impurity keeps the crust hot for a longer period of time. We find that  $Q_{\text{imp}} \simeq 8$  is allowed by the data, with no shallow heating needed and a core temperature of  $\tilde{T}_0 = 4 \times 10^6 \text{ K}$  (dotted curve in Figure 3). The crust then cools to  $kT_{\text{eff}}^{\infty} \simeq 24 \text{ eV}$  in  $\simeq 2 \text{ yr}$ . For  $Q_{\text{imp}} > 8$  the temperature curves overshoot our data.

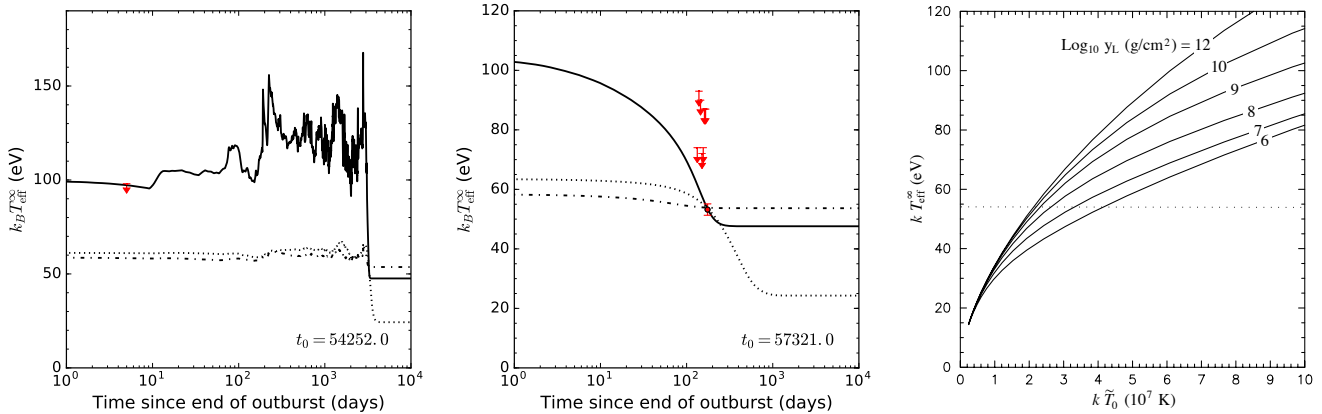


**Figure 3.** Left and middle: Three different thermal evolution simulations of HETE J1900.1–2455 that account for flux variations during outburst, along with the *Chandra* temperature measurement and *Swift* upper limits. On the left the evolution during and after the brief 2007 quiescence epoch and in the middle the evolution in quiescence in 2015–2016. Right: The observed effective temperature  $T_{\text{eff}}^{\infty}$  as a function of the red-shifted core temperature  $\tilde{T}_0$  (assuming  $M = 1.4 M_{\odot}$  and  $R = 10$  km) for varying depth of the light element envelope  $y_L$ . The horizontal dotted line shows the 2016 *Chandra* measurement of  $T_{\text{eff}}^{\infty}$ .

A single impurity parameter for the entire crust is likely not a correct assumption (e.g. Page & Reddy 2013). Theoretically, one expects  $Q_{\text{imp}}$  to be high at low densities due to the mixture of elements created during thermonuclear X-ray bursts (e.g. Schatz et al. 1999; Horowitz et al. 2007; Roggero & Reddy 2016). However, after crossing the neutron drip density ( $\rho_{\text{drip}} \simeq 6 \times 10^{11} \text{ g cm}^{-3}$ ), neutrons can be exchanged between nuclei and hence  $Q_{\text{imp}}$  likely decreases (e.g. Gupta et al. 2008; Steiner 2012). Therefore, we also calculated a model with an impurity parameter that changes at the neutron drip density. We fixed  $Q_{\text{imp}} = 1$  at high density and then searched for the maximum allowable impurity parameter at low density that fits the data. The resulting model, without a shallow heat source, has  $Q_{\text{imp}}^{\text{low}} = 28$  and  $\tilde{T}_0 = 4 \times 10^6$  K. The cooling curve looks very similar to our model for  $Q_{\text{imp}} = 8$  (dotted curve in Figure 3), and therefore we do not show it separately.

Since we cannot fully exclude that HETE J1900.1–2455 continued to accrete just below the *MAXI* detection limit, we also calculated models with  $t_0$  set to MJD 57454, which corresponds to the first *Swift*/XRT non-detection on 2016 March 7. For  $Q_{\text{imp}} = 1$ , the allowed shallow heating ( $Q_{\text{sh}} \simeq 2$  MeV) and core temperature ( $\tilde{T}_0 = 1.5 \times 10^7$  K) are both lower than for  $t_0$  set to MJD 57321, and further cooling to  $kT_{\text{eff}}^{\infty} \simeq 45$  eV would be expected.

## 5 DISCUSSION

We report on *Chandra* and *Swift* observations obtained within  $\simeq 180$  d after the  $\simeq 10$ -yr long outburst of the neutron star LMXB and intermittent AMXP HETE J1900.1–2455. Analysis of the *Chandra* data reveals that the quiescent spectrum is dominated by soft, thermal emission that can be described by a neutron star atmosphere model with a temperature of  $kT_{\text{eff}}^{\infty} \simeq 54$  eV. Any hard emission tail contributes  $\lesssim 9$  per cent to the total 0.5–10 keV luminosity of  $L_X \simeq 5 \times 10^{31} (D/4.7 \text{ kpc})^2 \text{ erg s}^{-1}$ , for an assumed power-law spectral shape with a photon index of  $\Gamma = 1 - 2$ .

HETE J1900.1–2455 is different from the AMXPs by exhibiting a thermally-dominated quiescent X-ray spectrum. Other AMXPs (both persistently and intermittently pulsating) display strong power-law emission, contributing  $\gtrsim 50\%$  to the total unab-

sorbed quiescent 0.5–10 keV flux (e.g. Campana et al. 2005; Wijnands et al. 2005b; Heinke et al. 2009; Degenaar et al. 2012).

With regard to the quasi-persistent neutron star LMXBs, HETE J1900.1–2455 is much colder after its long outburst than other sources observed at a similar epoch ( $kT_{\text{eff}}^{\infty} \gtrsim 90$  eV; e.g. Wijnands et al. 2001, 2002, 2003, 2004; Degenaar et al. 2011b; Fridriksson et al. 2010; Homan et al. 2014). Moreover, our thermal evolution calculations indicate that the crust of the neutron star in HETE J1900.1–2455 fully cools in  $\simeq 0.5$ –2 yr, which is short compared to the years-long cooling seen for other quasi-persistent sources (e.g. Cackett et al. 2013; Fridriksson et al. 2011; Degenaar et al. 2014; Homan et al. 2014; Merritt et al. 2016).

Our thermal evolution simulations suggest that both the low post-outburst temperature and the relatively fast cooling time scale of HETE J1900.1–2455 may be due to its relatively low mass-accretion rate during outburst. Indeed, our inferred mass-accretion rate is a factor  $\simeq 2$  lower than that of the crust-cooling source EXO 0748–676, and a factor  $> 5$  lower than that of others (see table 1 in Degenaar et al. 2015, and references therein). For a lower mass-accretion rate, the crust is heated less strongly and its temperature is lower, resulting in a shorter cooling time-scale (see e.g. figure 1 in Page & Reddy 2013). Nevertheless, it is striking that with only a factor  $\simeq 2$  difference in mass-accretion rate, EXO 0748–676 was detected at  $kT_{\text{eff}}^{\infty} \simeq 115$  eV at  $\simeq 180$  days after its  $\simeq 24$ -yr long outburst (Degenaar et al. 2011b). This likely points to other differences between these two sources, e.g. contrasting core temperatures or different crust properties.

Notably, HETE J1900.1–2455 is the only quasi-persistent LMXB that acted as an AXMP, and the disappearance of its pulsations has been explained as its magnetic field being “buried” by accretion (e.g. Cumming 2008; Patruno 2012). It is currently unclear if/how this should affect the thermal properties. If the magnetic field is strongly folded into the crust so that it reaches  $\simeq 10^{11}$  G, it may create an insulating layer that prevents the accretion-induced heat to propagate to the surface until the magnetic field re-emerges. If so, the neutron star temperature (and perhaps any hard emission) could possibly increase after the Ohmic diffusion timescale. This could be as short as tens of days for HETE J1900.1–2455 (e.g. Cumming 2008). Nevertheless, our work suggests that the quiescent data obtained so far can be explained with similar physical

parameters as inferred for other crust-cooling sources. At present there are thus no indications that its magnetic field has a notable impact its thermal properties.

Our simulations show that if the crust of the neutron star is highly conductive with  $Q_{\text{imp}} = 1$ , no further cooling is expected in HETE J1900.1–2455. Our *Chandra* measurement then reflects the temperature of the neutron star core,  $\tilde{T}_0 \simeq 2 \times 10^7$  K. However, the present data allow for a higher impurity parameter, up to  $Q_{\text{imp}} \simeq 8$ , for which the core temperature may be as low as  $\tilde{T}_0 \simeq 4 \times 10^6$  K and further cooling of the crust is expected. Future observations of HETE J1900.1–2455 in quiescence can thus further constrain the impurity of the crust and temperature of the core, as well as possible effects of the magnetic field on the thermal properties.

The total energy released during the  $\simeq 10$  yr accretion outburst, from both the standard nuclear processes and additional shallow heating, amount to  $\simeq 2 \times 10^{43}$  erg. As the present work was in progress, Cumming et al. (2016) found that such an amount of energy can raise the core temperature and provides us with a lower limit on its heat capacity that depends on the tantalizing core composition. Comparing with their figure 7, our  $\tilde{T}_0 \simeq 2 \times 10^7$  K provides the strongest constraint to date on the core heat capacity: it must be  $C > 10^{37} (\tilde{T}_0/10^8 \text{ K}) \text{ erg K}^{-1}$ , a value that is close to the minimum provided by the leptons in the core. This minimum can only be reached if all baryons are strongly paired, i.e. superfluid or superconducting, hence have a negligible contribution to the total heat capacity. Observing further cooling in HETE J1900.1–2455 would push this lower limit further down and may limit the maximum fraction of baryons that are paired, and consequently the minimum fraction of baryons that are not paired.

## ACKNOWLEDGEMENTS

We are grateful to the *Chandra* team for making this DDT observation possible and to the referee for valuable comments. We acknowledge the use of *Swift* public data archive. ND is supported via an NWO Vidi grant and EU Marie Curie Intra-European fellowship. RW and LO are supported by an NWO Top grant, module I, awarded to RW. DP is partially supported by the Consejo Nacional de Ciencia y Tecnología with a CB-2014-1 grant #240512.

## REFERENCES

- Brown E., Cumming A., 2009, *ApJ*, 698, 1020  
 Brown E., Bildsten L., Rutledge R., 1998, *ApJ*, 504, L95  
 Cackett E., Brown E., Cumming A., Degenaar N., Fridriksson J., Homan J., Miller J., Wijnands R., 2013, *ApJ*, 774, 131  
 Campana S., Colpi M., Mereghetti S., Stella L., Tavani M., 1998, *A&ARv*, 8, 279  
 Campana S., Ferrari N., Stella L., Israel G., 2005, *A&A*, 434, L9  
 Campana S., Stella L., Israel G., D’Avanzo P., 2008, *ApJ*, 689, L129  
 Chakrabarty D. et al., 2014, *ApJ*, 797, 92  
 Cumming A., 2008, in R. Wijnands, D. Altamirano, P. Soleri, N. Degenaar, N. Rea, P. Casella, A. Patruno, M. Linares, eds, *AIP Conf. Ser. Vol.1068. Am. Inst. Phys., New York*, p. 152  
 Cumming, A., Brown, E. F., Fattoyev, F. J., Horowitz, C. J., Page, D., Reddy, S., 2016, arXiv:1608.07532,  
 Degenaar N., Brown E., Wijnands R., 2011a, *MNRAS*, 418, L152  
 Degenaar N., Patruno A., Wijnands R., 2012, *ApJ*, 756, 148  
 Degenaar N. et al., 2007a, *Astron. Telegram*, 1091  
 Degenaar N. et al., 2007b, *Astron. Telegram*, 1098  
 Degenaar N. et al., 2007c, *Astron. Telegram*, 1106  
 Degenaar N. et al., 2011b, *MNRAS*, 412, 1409  
 Degenaar N. et al., 2014, *ApJ*, 791, 47  
 Degenaar N. et al., 2015, *MNRAS*, 451, 2071  
 Deibel A., Cumming A., Brown E. F., Page D., 2015, *ApJ*, 809, L31  
 Elshamouty K., Heinke C., Morsink S., Bogdanov S., Stevens A., 2016, *ApJ*, 826, 162  
 Fridriksson J. et al., 2010, *ApJ*, 714, 270  
 Fridriksson J. et al., 2011, *ApJ*, 736, 162  
 Galloway D., Morgan E., Chakrabarty D., Kaaret P., 2007, *Astron. Telegram*, 1086  
 Galloway D., Muno M., Hartman J., Psaltis D., Chakrabarty D., 2008a, *ApJS*, 179, 360  
 Galloway D. K., Morgan E. H., Chakrabarty D., 2008b, in R. Wijnands, D. Altamirano, P. Soleri, N. Degenaar, N. Rea, P. Casella, A. Patruno, M. Linares, *AIP Conf. Ser. Vol.1068. Am. Inst. Phys., New York*, p. 55  
 Gehrels N., 1986, *ApJ*, 303, 336  
 Gupta S. S., Kawano T., Möller P., 2008, *Phys. Rev. Lett.*, 101, 231101  
 Haensel P., Zdunik J., 1990, *A&A*, 227, 431  
 Haensel P., Zdunik J., 2008, *A&A*, 480, 459  
 Heinke C., Rybicki G., Narayan R., Grindlay J., 2006, *ApJ*, 644, 1090  
 Heinke C., Jonker P., Wijnands R., Deloye C., Taam R., 2009, *ApJ*, 691, 1035  
 Homan J., Fridriksson J. K., Wijnands R., Cackett E. M., Degenaar N., Linares M., Lin D., Remillard R. A., 2014, *ApJ*, 795, 131  
 Horowitz C., Berry D., Brown E., 2007, *Phys. Rev. E*, 75, 066101  
 Horowitz C. J., Berry D. K., Briggs C. M., Caplan M. E., Cumming A., Schneider A. S., 2015, *Physical Review Letters*, 114, 031102  
 Jonker P., Campana S., Steeghs D., Torres M., Galloway D., Markwardt C., Chakrabarty D., Swank J., 2005, *MNRAS*, 361, 511  
 Kaaret P., Morgan E. H., Vanderspek R., Tomsick J. A., 2006, *ApJ*, 638, 963  
 Krimm H. et al., 2013, *ApJS*, 209, 14  
 Lattimer J. M., 2011, *A&AS*, 336, 67  
 Matsuoka et al. M., 2009, *PASJ*, 61, 999  
 Medin Z., Cumming A., 2014, *ApJ*, 783, L3  
 Merritt R. L. et al., 2016, arXiv:1608.03880  
 Ootes L. S., Page D., Wijnands R., Degenaar N., 2016, *MNRAS*, 461, 4400  
 Page D., Reddy S., 2013, *Phys. Rev. Lett.*, 111, 241102  
 Patruno A., 2012, *ApJ*, 753, L12  
 Potekhin, A. Y., Chabrier, G., Yakovlev, D. G., 1997, *A&A*, 323,415  
 Roggero A., Reddy S., 2016, *Phys. Rev. C*, 94, 5803  
 Rutledge R., Bildsten L., Brown E., Pavlov G., Zavlin V., 2001, *ApJ*, 559, 1054  
 Rutledge R., Bildsten L., Brown E., Pavlov G., Zavlin V., Ushomirsky G., 2002, *ApJ*, 580, 413  
 Schatz H., Bildsten L., Cumming A., Wiescher M., 1999, *ApJ*, 524, 1014  
 Shternin P., Yakovlev D., Haensel P., Potekhin A., 2007, *MNRAS*, 382, L43  
 Steiner, A. W., 2012, *Phys. Rev. C*, 85, 055804  
 Turlione A., Aguilera D. N., Pons J. A., 2015, *A&A*, 577, A5  
 Vanderspek R., Morgan E., Crew G., Graziani C., Suzuki M., 2005, *Astron. Telegram*, 516  
 Verner D., Ferland G., Korista K., Yakovlev D., 1996, *ApJ*, 465, 487  
 Wachter K., Leach R., Kellogg E., 1979, *ApJ*, 230, 274  
 Waterhouse A. C., Degenaar N., Wijnands R., Brown E. F., Miller J. M., Altamirano D., Linares M., 2016, *MNRAS*, 456, 4001  
 Wijnands R., van der Klis M., 1998, *Nature*, 394, 344  
 Wijnands R., Miller J., Markwardt C., Lewin W., van der Klis M., 2001, *ApJ*, 560, L159  
 Wijnands R., Guainazzi M., van der Klis M., Méndez M., 2002, *ApJ*, 573, L45  
 Wijnands R., Nowak M., Miller J., Homan J., Wachter S., Lewin W., 2003, *ApJ*, 594, 952  
 Wijnands R., Homan J., Miller J., Lewin W., 2004, *ApJ*, 606, L61  
 Wijnands R., Homan J., Heinke C., Miller J., Lewin W., 2005b, *ApJ*, 619, 492  
 Wijnands R., Degenaar N., Armas Padilla M., Altamirano D., Cavecchi Y., Linares M., Bahramian A., Heinke C. O., 2015, *MNRAS*, 454, 1371  
 Wilms J., Allen A., McCray R., 2000, *ApJ*, 542, 914